Published in final edited form as:
Biomacromolecules. 2014 January 13; 15(1): 132–142. doi:10.1021/bm401413c.

Synthesis, Physicochemical Characterization, and Cytocompatibility of Bioresorbable, Dual-Gelling Injectable Hydrogels

Tiffany N. Vo, **Adam K. Ekenseair**, **F. Kurtis Kasper**, and **Antonios G. Mikos***
Department of Bioengineering, Rice University, Houston, TX, 77030, USA

Abstract

Injectable, dual-gelling hydrogels were successfully developed through the combination of physical thermogellation at 37°C and favorable amine:epoxy chemical crosslinking. Poly(*N*-isopropylacrylamide)-based thermogelling macromers with a hydrolyzable lactone ring and epoxy pendant groups, and a biodegradable diamine-functionalized polyamidoamine crosslinker were synthesized, characterized, and combined to produce non-syneresing and bioresorbable hydrogels. Differential scanning calorimetry and oscillatory rheometry demonstrated the rapid and dual-gelling nature of the hydrogel formation. The post-gelation dimensional stability, swelling, and mechanical behavior of the hydrogel system were shown to be easily tuned at the synthesis and formulation stages. The leachable products were found to be cytocompatible at all conditions, while the degradation products demonstrated a dose- and time-dependent response due to solution osmolality. Preliminary encapsulation studies showed MSC viability could be maintained for 7 days. The results suggest that injectable, thermally and chemically crosslinkable hydrogels are promising alternatives to prefabricated biomaterials for tissue engineering applications, particularly for cell delivery.

Keywords

injectable hydrogel; poly(*N*-isopropylacrylamide); tissue engineering; thermogelling

1. Introduction

Injectable, *in situ* forming hydrogels are a promising alternative to implantable prefabricated scaffolds investigated for craniofacial tissue engineering. Due to their ability to form three-dimensional, highly hydrated substrates in a minimally invasive manner, this versatile class of polymer-based biomaterials can enable local delivery of growth factors and cells, can easily create scaffolds that fill and conform to complex configurations, and provide a supportive environment for cell migration and proliferation. The benefits of and approaches towards designing injectable hydrogels for tissue engineering have been recently reviewed[1–6].

*Corresponding author. mikos@rice.edu.

Supporting Information Available

Supplementary Figure 1. Gelation of TGM and crosslinked TGM 10 wt % hydrogels with P-1440 crosslinker at 1:1 amine:epoxy mol ratio at 37°C after 1 h (left column) and 4°C in excess PBS pH 7.4 after 3 h (right column). TGM only hydrogels displayed syneresis and reversible gelation (red arrow) when transferred to 4°C, fully solubilizing after 12 h (data not shown). Crosslinked hydrogels turned transparent with a yellow tint due to the PAMAM after 1 h, and maintained their cylindrical shape in the absence of thermogelation (orientation and shape designated by the dotted line cylinder). This material is available free of charge via the Internet at http://pubs.acs.org.

Thermoresponsive polymers are particularly attractive injectable materials, since gelation to a physically crosslinked hydrogel is triggered solely by temperature elevation to and above the lower critical solution temperature (LCST). Hydrogels based on one polymer, poly(*N*-isopropylacrylamide) (PNiPAAm), have been widely investigated for various biomedical applications, as it undergoes a sol-gel transition at its LCST of 32°C[7]. Previous work has determined various means to tune and modulate the gelation kinetics[8] and has demonstrated controlled environmentally-responsive drug and growth factor delivery[9, 10]. Additionally, PNiPAAm-based hydrogels have been successfully used for the encapsulation of articular chondrocytes *in vitro*[11]. However, the main challenges associated with PNiPAAm-based hydrogels have been syneresis and non-degradability, limiting their efficacy for tissue engineering applications. Syneresis, or shrinkage of the hydrogel over time, can reduce nutrient diffusion to encapsulated cells. Additionally, hydrogel shrinkage would minimize hydrogel-tissue contact within the defect, impeding tissue integration. Biodegradation is also important, as non-degradable materials present a physical barrier to further tissue repair and increase the chances of an inflammatory response. Thus, rational design of PNiPAAm hydrogels to address both factors can drastically advance the properties of these materials for controlled delivery and improved integration in tissue engineering applications[12].

A number of groups have attempted to enhance bioresorbability of PNiPAAm polymers by copolymerizing complex pendant groups such as lactate ester[13, 14] or polyester[15] side groups, 2-methylene-1,3-dioxepane[16], poly(amino acid)[17], or 2-hydroxyethylmethacrylate-6-hydroxyhexanoate[18] that modulate the LCST over time. The materials became increasingly resorbable when the LCST of the polymer rose sufficiently above body temperature. In these cases involving polyesters, lactate side chains, or poly(amino acids), the monomers also produced soluble degradation products that may be toxic to encapsulated cells and raise the pH of the local microenvironment. In a different study, Cui *et al.* achieved PNiPAAm biodegradation without toxic byproducts through incorporation of dimethyl-γ-butyrolactone acrylate (DBA), a hydrolyzable lactone ring[19, 20]. Hydrolysis of the ester group in the ring structure resulted in the formation of hydroxyl and carboxyl groups, which increased the hydrophilicity, and subsequently, the LCST of the polymer. Cui *et al.* demonstrated that the pre- and post-hydrolysis LCST was linearly controlled with the DBA mol content[20] and could be tuned with addition of other hydrophilic comonomers[19].

Our laboratory has previously reported the development of a novel class of PNiPAAm-based hydrogels with dual gelation mechanisms to create non-shrinking, thermally responsive, and chemically crosslinked hydrogels for craniofacial tissue engineering applications[21, 22]. The two component system consisted of a non-degradable thermogelling macromer (TGM) with epoxy pendant rings and a water soluble, hydrolytically degradable, diamine-functionalized polyamidoamine (PAMAM) crosslinker. The macromer was designed to rapidly form physically crosslinked hydrogels slightly below physiological temperature, followed by slower chemical crosslinking *in situ* through the epoxy ring – amine group reaction. The main advantage of this system is that the thermal gelation and favorable epoxy crosslinking reaction occur through mild processes and require no exogenous, cytotoxic initiators, thus allowing for cell delivery in irregular shaped, non-loading bearing defects such as in the craniofacial bone. Syneresis of the hydrogels was eliminated in a PAMAM concentration-dependent manner[22], and extensive *in vitro* testing demonstrated the tunability of the hydrogel parameters and hydrolytic degradation under accelerated conditions to achieve targeted material properties and partially soluble degradation products, respectively[21].

In order to improve upon the previous hydrogel system and enable the hydrophobic TGM chains to be more readily cleared from the body, the objective of this study was to develop and characterize injectable, thermally responsive, chemically crosslinkable, and fully

bioresorbable hydrogels comprising TGMs based on PNiPAAm, glycidyl methacrylate (GMA), DBA, and acrylic acid (AA) and diamine-functionalized PAMAM crosslinkers. Physical and chemical crosslinking would be achieved via thermogelation of the PNiPAAm upon temperature elevation to 37°C and favorable crosslinking of the GMA pendant epoxy rings with the amine groups of the PAMAM crosslinker. Time-dependent degradation of hydrogel would be accomplished through the incorporation of the DBA hydrolyzable lactone ring, which would enable the polymer to resolubilize over time via LCST modulation. Lastly, the addition of hydrophilic AA compensated for the hydrophobicity of both the GMA and DBA comonomers and tuned the initial LCST between room and physiologic temperature. We hypothesized that the copolymerization of NiPAAm, a chemically crosslinkable epoxy pendant group and hydrolyzable lactone ring, allowing for the modulation of the LCST *in situ*, would produce non-shrinking, injectable hydrogels with fully soluble degradation products. The effects of LCST modulation by DBA content and varying hydrogel parameters on the physicochemical properties, material behavior and *in vitro* cytocompatibility were evaluated. Additionally, a preliminary encapsulation was performed with mesenchymal stem cells (MSCs) to evaluate the hydrogel's potential for cell delivery in tissue engineering applications.

2. Materials and Methods

2.1 Materials

NiPAAm, DBA, GMA, AA, 2,2'-azobis(2-methylpropionitrile) (azobisisobutyronitrile, AIBN), *N*,*N*'-methylenebisacrylamide (MBA), and piperazine (PiP) were purchased from Sigma Aldrich (Sigma, St. Louis, MO) and used as received. Anhydrous 1,4-dioxane, diethyl ether, and acetone in analytical grade; water, acetonitrile, chloroform, and methanol in HPLC-grade; and 1 N sodium hydroxide (NaOH) were purchased from VWR (Radnor, PA) and used as received. PBS (powder, pH 7.4) was obtained from Gibco Life, Grand Island, NY. Ultrapure water was obtained from a Millipore Super-Q water system (Millipore, Billerica, MA).

2.2 TGM Synthesis and Characterization

Synthesis of P(NiPAAm-*co*-GMA-*co*-DBA-*co*-AA) TGM was performed according to established protocols[19, 22], as shown in Scheme 1. In a typical reaction, 10 g of NiPAAm, GMA, DBA and AA was dissolved in anhydrous 1,4-dioxane under nitrogen at 65°C. AIBN in dioxane was added at 0.7% of total mol content to initiate free radical polymerization and the reaction mixture was stirred for 16 h. After solvent removal by rotary evaporation, the material was re-dissolved in acetone and purified twice via dropwise precipitation in excess diethyl ether. The recovered polymer was air-dried overnight and transferred to a vacuum oven for several days prior to elemental analysis. The chemical composition of the TGMs was determined by proton nuclear magnetic resonance spectroscopy (400 MHz ^{1}H NMR, Bruker, Switzerland). The polymer was dissolved in D_2O at a concentration of 20 mg/mL that contained 0.75 wt % 3-(trimethylsilyl)propionic-2,2,3,3-d_4 acid, sodium salt as an internal shift reference (Sigma-Aldrich, St. Louis, MO) and the data were analyzed using the MestRe-C NMR software package (Mestrelab Research S.L., Spain) and quantitative NMR analysis. Acid titration was performed in conjunction with ^{1}H NMR to determine the AA content of the TGMs before hydrolysis. Aqueous gel permeation chromatography (GPC) using a Waters Alliance HPLC system (Milford, MA) and differential refractometer (Waters, model 410) equipped with a series of analytical columns (Waters Styragel guard column 20 mm, 4.6 × 30 mm; Waters Ultrahydrogel column 1000, 7.8 × 300 mm) was used to determine the molecular weight distributions of the synthesized TGMs[23]. The TGM was first hydrolyzed in accelerated conditions (see *Before and After Hydrolysis LCST* section) to remove its thermogelling properties. The weight average molecular weight (M_w), number

average molecular weight (M_n), and polydispersity index (PDI = M_w/M_n) of the hydrolyzed polymer were determined by comparison to commercially available narrowly dispersed molecular weight poly(ethylene glycol) (PEG) standards (Waters, Mississauga, ON).

2.3 PAMAM Synthesis and Characterization

PAMAM was synthesized by the polyaddition of PiP and MBA at a stoichiometric ratio of [MBA]/[PiP] = 0.75 or 0.85 following previously reported protocols[22]. Molecular weight distributions of the synthesized PAMAM crosslinkers were analyzed using time-of-flight mass spectroscopy with positive-mode electrospray ionization on a Bruker microTOF ESI spectrometer (Bruker Daltonics, Billerica, MA) equipped with a 1200 series HPLC (Agilent Technologies, Santa Clara, CA) to deliver the mobile phase (50:50 HPLC-grade water and methanol). After data acquisition, all peaks (including degradation and secondary reaction products) were identified using microTOF Control software (Bruker) following published procedures[22]. The peaks were corrected for charge state (generally with H^+ or Na^+ and rarely K^+ ions), and quantified for calculation of M_n, M_w, and PDI.

2.4 Before and After Hydrolysis LCST

The LCSTs of the TGMs before and after hydrolysis were determined by differential scanning calorimetry (DSC). Unhydrolyzed and hydrolyzed polymers were dissolved in PBS pH 7.4 to create 10 wt % solutions. Hydrolyzed polymers were created by dissolving TGM in ultrapure water or PBS pH 7.4 at 4°C in 4 mL glass vials followed by addition of 50 μL of 0.1 N NaOH solution. The solutions were dialyzed against water and were used immediately for DSC.

14 μL of each polymer solution was pipetted into an aluminum volatile sample pan (TA Instruments, Newcastle, DE) and capped/crimped. Thermograms were recorded on a TA Instruments DSC 2920 equipped with a refrigerated cooling system against an empty sealed pan as reference. The oven was equilibrated at 5°C for 10 min and then heated to 80°C at a heating rate of 5°C/min. The LCST was determined both as the onset and peak temperature of the endothermic peak in the thermogram using the Universal Analysis 2000 software provided with the DSC system.

2.5 Hydrogel Fabrication

Hydrogels (6 mm in diameter, 3 mm in height) were fabricated by combining the TGM and PAMAM crosslinker. Individual solutions of TGM and PAMAM crosslinker were prepared at twice the desired concentrations in PBS pH 7.4 and placed on a shaker table at 4°C until dissolved. The PAMAM solution was pipetted into the TGM solution using cold pipet tips and the resulting solution was manually mixed in the glass vial. 90 μL injections were transferred to 6 mm diameter × 3 mm height cylindrical Teflon molds at 37°C and allowed to gel for 24 h. To evaluate the macroscopic properties of the hydrogel system, the hydrogels were fabricated as stated in the above section, except that after manual mixing, the glass vial was transferred to a water bath at 37°C for immediate observation of the thermogelling properties. Syneresis was qualitatively evaluated after 24 h at 37°C.

2.6 Rheological Characterization

A thermostatted, oscillating rheometer (Rheolyst AR1000, TA Instruments, New Castle, DE) equipped with a 6 cm steel cone (1 degree) with a gap size of 26 μm at a frequency of 1 Hz and displacement of 1×10^{-4} rad was used to evaluate the elastic response of the hydrogels. Hydrogel formulations in pH 7.4 PBS were pipetted onto the rheometer, and the dynamic viscoelastic properties of the solutions, namely, the dynamic shear storage (G') and loss (G") moduli, complex viscosity (|η*|), and loss angle (δ), were recorded using the TA

Rheology Advantage software (TA Instruments). The solution was maintained at 4°C followed by elevation to and maintenance at 37°C for 3 h to monitor the crosslinking reaction.

2.7 *In Vitro* Degradation

Accelerated degradation studies were performed in accordance with ISO 10993 standards[24]. Hydrogels were fabricated in 6 mm diameter × 3 mm height cylindrical Teflon molds. Hydrogels were weighed at formation (W_f) and then frozen and lyophilized. After initial dry weight was measured (W_i), gels were reswollen in 4 mL glass vials with 4 mL of PBS pH 10.5 at 70°C, and weekly solution changes were performed. At each timepoint, the samples (n = 6) were carefully blotted, weighed (W_s) and lyophilized. The dry weight was measured (W_d) and percent of polymer loss was calculated through the difference between the initial and final dry weights divided by the initial dry mass ($(W_i\text{-}W_d)/W_i*100$)[25].

2.8 Hydrogel Swelling

Hydrogel swelling behavior was assessed in a 2^4 factorial experimental design with formulations of varying TGM wt %, DBA mol content, PAMAM molecular weight, and amine:epoxy mol ratio. The individual solutions were fabricated as previously described in 6 mm diameter × 3 mm height cylindrical molds at 37°C. After 24 h, the hydrogels were weighed on a balance and placed in excess PBS for 24 h at 37°C. Hydrogels were then weighed after swelling, frozen at −80°C, lyophilized and reweighed when dry. The hydrogel swelling ratio at formation ($q_{formation}$) and equilibrium ($q_{equilibrium}$) were calculated as the difference between the swollen and dry mass divided by the dry mass[25].

2.9 Mechanical Testing

Hydrogel formulations with varying TGM wt % and amine:epoxy mol ratio (n = 6 per group) were fabricated as previously described. Mechanical testing on a TA Instruments Thermomechanical Analyzer 2940 (TA Instruments, Newcastle, DE) equipped with a wide compression probe (diameter of 6 mm) was performed to assess the unconfined compressive Young's modulus of the hydrogels. Samples were first placed onto the prewarmed stage, and sample height was measured by the probe. The stage was then re-equilibrated to 37°C and the sample was compressed at a rate of 0.001 N/min to 0.05 N. The unconfined Young's modulus was determined to be the initial slope of the engineering strain versus engineering stress curve.

2.10 Cytocompatibility Testing

2.10.1 Cell Culture—A rat fibroblast cell line (ATCC, CRL-1764) was chosen for the *in vitro* cytocompatibility tests. The cells were cultured on T-75 flasks using Dulbecco's modified Eagle medium (DMEM; Gibco Life, Grand Island, NY) supplemented with 10% (v/v) fetal bovine serum (FBS; Cambrex BioScience, Walkersville, MD) and 1% (v/v) antibiotics containing penicillin, streptomycin and amphotericin (Gibco Life). Cells were cultured in a humidified incubator at 37°C and 5% CO_2. Cells of passage number 3–5 were used.

2.10.2 *In Vitro* Cytocompatibility—The leachables and degradation products assays for cytocompatibility were performed following established protocols[22, 26, 27]. Solutions of hydrogels were prepared at the appropriate concentrations by dissolving TGM and PAMAM in serum-free DMEM at 4°C. The hydrogels were fabricated in 6 mm diameter × 3 mm height Teflon molds and allowed to gel for 24 h in a 37°C incubator. Hydrogels were then processed for the leachables or degradation products assay and the test media were diluted to 1, 10, and 100 times original concentration. Cultured fibroblasts were passaged at 80–90%

confluency and 96-well plates were seeded at a cell density of 10,000 cells/well and cultured for 24–48 h until 90% confluent. The test media and its dilutions were fed at 100 μL/well to the cells (n = 6), replacing the original media, and incubated for two established timepoints, 2 or 24 h[22, 26, 27], at 37°C, 95% relative humidity, and 5% CO_2. Cells fed serum-free media (without polymer) served as a positive (live) control and cells exposed to 70% ethanol for 10 min were used as a negative (dead) control.

After incubation, the test media were removed and the cells were rinsed three times with pH 7.4 PBS before adding calcein AM and ethidium homodimer-1 at 2 μM and 4 μM concentrations in PBS, respectively (Live/Dead viability/cytotoxicity kit, Molecular Probes, Eugene, OR). The cells were incubated in the dark at room temperature for 30 min. Cell viability was quantified using a fluorescence plate reader (Biotek Instrument FLx800, Winooski, VT) equipped with filter sets of 485/528 nm (excitation/emission) for calcein AM (live cells) and 528/620 nm (excitation/emission) for EthD-1 (dead cells). The fluorescence of the cell populations was recorded and the fractions of live and dead cells were calculated relative to the controls.

2.10.3 Leachables Assay—For the leachables assay, hydrogels were incubated in serum-free media for 24 h in a 37°C warm room at a 3 cm^2/mL surface area:volume ratio according to established procedures[26]. The test media were then sterile filtered and incubated with the cells.

2.10.4 Degradation Products Assay—For the degradation products study, hydrogels were placed in ultrapure water with 2 mL of 1 N NaOH solution at 37°C until fully degraded. Dialysis was not performed on the solution, as the degradation products may range in molecular weight. The solution with the complete degradation products was frozen at −80°C, lyophilized, reconstituted into the same volume of serum-free media required for fabrication, and sterile filtered prior to cell exchange.

2.10.5 Ion Concentration Cytocompatibility—To isolate the effects of solution osmolality from the degradation products, media with 0, 30, 60, 90, 120, and 220 mg NaCl/10 mL DMEM were measured via osmometry, sterile filtered, incubated with cells, and viability was recorded at 24 h (n = 6). NaCl was chosen as a biocompatible molecule that would allow for isolation of the effects of osmolality without introducing any effects of pH or molecular composition on cell viability. The quantity of NaCl added was calculated to be the theoretical amount of NaCl salt to raise a 10 mL media solution by 100 mOsm.

2.10.6 Osmolality Determination—Solution osmolality was determined by measurement with an Osmette A Automatic Osmometer (Precision Systems, Inc., Natick, MA) calibrated with 100 and 500 mOsm/kg H_2O standard solutions (Precision Systems, Inc.) and run on the 0 – 2k mOsm range.

2.11 MSC Encapsulation

An encapsulation study was performed to demonstrate the cell delivery capabilities of the hydrogel. MSCs were harvested from rat femora and tibiae of 6–8 week old Fisher 344 rats (Charles River Laboratories, Wimington, MA) following established procedures in accordance to approved protocols by the Rice Institutional Animal Care and Use Committee[28]. The rats were euthanized by CO_2 asphyxiation and a bilateral thoracotomy following anesthesia using 4% isofluorane/O_2 mixture (Baxter Healthcare, Deerfield, IL). The tibiae and femora were aseptically removed, placed in Dulbecco's modified Eagle's medium (Invitrogen, Carlsbad, CA) with 10% fetal bovine serum (FBS) (Cambrex Bioscience) and 3% penicillin-streptomycin-fungizone (Invitrogen), and flushed with

complete osteogenic medium containing minimum essential medium Eagle-alpha modification (Invitrogen), 10% FBS, 10 mM b-glycerol-2-phosphate, 50 mg/L ascorbic acid and 1% penicillin-streptomycin-fungizone (Invitrogen). The marrow pellets were broken up, sterile filtered and plated in 75 cm^2 tissue culture flasks at 37°C under humidified, 5% CO_2 atmosphere with complete osteogenic media containing 10^{-8} M dexamethasone. TGM and PAMAM polymers were UV sterilized for 3 h and dissolved in PBS pH 7.4 as previously described. After 6 days of culture, the MSCs were passaged and added to the polymer solutions at a final concentration of 10 million cells/mL hydrogel. The solution was manually mixed, pipetted into 8 mm × 2 mm autoclaved Teflon molds on a heat block, and allowed to crosslink at 37°C in an incubator. After 2.5 h, the hydrogels and their acellular controls were placed in 2.5 mL media in 12-well tissue culture plates and cultured for 1 and 7 days. At each timepoint, the hydrogels were soaked in PBS for 30 min, sliced in half, weighed, and processed for DNA Picogreen assay (n = 4 halves) and Live/Dead confocal imaging (n = 2 halves).

2.12 Statistics

The data are presented as mean ± standard deviation in triplicate, unless otherwise stated. The cytocompatibility data were analyzed via Tukey's post-hoc test ($p<0.05$) within timepoints and a t-test across timepoints ($p<0.05$). Main effects and interaction analysis of hydrogel swelling in the full 2^4 factorial experimental design were performed with JMP v.10 statistics software (SAS Institute, Cary, NC).

3. Results and Discussion

3.1 TGM Synthesis and Characterization

Copolymers of NiPAAm with reactive functional moieties for chemical crosslinking and LCST modulation were successfully synthesized. The chemical composition of the TGMs was characterized by NMR. The ^{1}H NMR spectra of P(NiPAAm-*co*-GMA-*co*-DBA-*co*-AA) TGM is shown in Figure 1. The five pendant protons on GMA are found between 2.8 and 4.8 ppm, along with the isopropyl proton on NiPAAm (3.9 ppm). The three protons on DBA are found at the double peak at 5.6 and 5.8 ppm and the single peak at 4.2 ppm, correlating to the relative peaks of the DBA comonomer (data not shown). The six NiPAAm methyl protons were located from 0.9–1.3 ppm and the remaining polymer backbone protons are located from 1.3 to 2.3 ppm. The relative locations of the peaks correlate similarly to those of PNiPAAm homopolymer, GMA monomer (data not shown) and similar PNiPAAm-DBA copolymers published in the literature[19, 20]. Calculations of the DBA mol content using the relative intensities of the DBA 2h protons gave an average value of 5.8 ± 0.3 % and 2.5 ± 0.3 %. The M_n, M_w, and PDI of the 6% DBA-containing TGM was found to be 56,100 ± 4600 Da, 113,600 ± 2500 Da, 2.02 ± 0.12, respectively, with the 2.5% DBA-containing TGM at similar values.

The before and after hydrolysis LCSTs of the TGMs were determined by DSC. The thermal properties of the synthesized TGM formulations are presented in Table 1. Copolymerization of NiPAAm with GMA and 6% or 2.5% DBA led to an initial peak LCST of 22.4 ± 1.0°C or 27.7 ± 0.1°C, respectively. This initial peak LCST is lower than the reported LCST of the PNiPAAM homopolymer (32°C) due to the hydrophobicity of the GMA and DBA comonomers. However, after hydrolysis of the ester groups in the ring to hydroxyl and carboxyl groups, the higher DBA content leads to an increase in hydrophilicity, which is associated with a higher LCST. Therefore, the 6% DBA TGM has a higher hydrolysis LCST of 63.3 ± 3.7°C compared to 39.5 ± 3.6°C for the 2.5% DBA TGM. The initial LCSTs determined by DSC corresponded with the macroscopically-observed thermogellation of the macromers and the reported hydrolysis of DBA in the literature[20].

3.2 PAMAM Synthesis and Characterization

Epoxy reactive PAMAM diamine crosslinkers with varied stoichiometric ratios were successfully synthesized and evaluated with ^{1}H NMR following established protocols[22]. MicroTOF was further performed to characterize the molecular weight distribution. Table 2 lists the composition of the two PAMAM diamine crosslinkers used for the following studies.

3.3 Hydrogel Fabrication

The TGM and PAMAM crosslinker were combined in PBS pH 7.4 to successfully form injectable, *in situ* forming hydrogels. The hydrogels were observed macroscopically to evaluate hydrogel gelation and post-formation syneresis. Upon mixing of the TGM and PAMAM solutions at 4°C and transfer to 37°C, the mixture began to thermogel instantaneously, as indicated by formation of an opaque white hydrogel. After a period of 30 min, the sol-gel transition was accompanied by a second color change in which the hydrogel became translucent. The crosslinking reaction was completed within 3 h, and, as hypothesized, a stable, non-shrinking hydrogel was observed compared to hydrogels formed by the TGM alone (Figure 2). Distinct rheological traces of the hydrogel crosslinking in the presence of thermogelation clearly demonstrate the dual gelling nature of the hydrogels (Figure 3). The 3 h run was stopped at 155 min after the adhesiveness of the hydrogel after crosslinking prevented further oscillation and accurate measurement. A rapid increase in the shear storage and loss moduli was observed in the initial 5 min of the trace, correlating to thermogelation at 37°C, followed by slower chemical crosslinking, which resulted in an ultimate shear storage modulus of 100 kPa. The storage modulus of the gel without chemical crosslinking peaks at about 100 kPa at 37°C; however, the thermodynamic instability of the hydrogels in the absence of chemical gelation results in a decreased storage modulus and complex viscosity in the subsequent 15–30 min at 37°C, which is observed in other studies[8].

The slight decrease in the first 15 min of the rheological trace is believed to be a result of the rapid loss in the thermogelling properties of the hydrogels due to a preferential hydrolysis of the DBA lactone ring at neutral and basic pH (data not shown). During the mixing of the TGM and PAMAM solutions, the PAMAM solution, which is basic, likely accelerated the hydrolysis of the DBA comonomer, leading to a loss in thermogelation at a faster rate than observed in previous studies[19]. This rapid change in LCST, while unexpected, simplified the degradation rate to be dependent only on PAMAM hydrolysis, which has been explored previously[21, 22]. Chemical gelation of the epoxy and amine groups in the absence of thermogelation was also performed via rheology similar to published studies[22]. While the interaction between the carboxylic acid groups of the TGM with the PAMAM crosslinkers is likely, as shown by other studies involving acids and amines[29], we hypothesize that due to the greater amount of amine and epoxy units and favorability of reaction[30, 31], the epoxy-amine reaction will dominate the crosslinking process. However, it was not possible to directly measure the crossover of the shear loss and shear storage moduli under the same conditions using rheology since the LCST of this system was lower, requiring a lower controlled temperature that would alter the hydrogel's original water content and crosslinking kinetics. Chemical crosslinking was macroscopically observed in the absence of thermogelation by the maintenance of the hydrogel shape after transfer to a 4°C environment (Supplementary Figure 1).

3.4 Accelerated Degradation

In vitro degradation studies were performed using 10 wt % hydrogels with 6% DBA and 1440 Da PAMAM at a 1:1 amine:epoxy ratio in basic accelerated conditions (PBS pH 10.5 at 70°C). Degradation was calculated as percent dry polymer mass loss over time. Figure 4 shows that the hydrogels fully degraded under accelerated conditions over 30 days. The 30%

weight loss after one day is attributed to the loss of sol fraction after incubation in PBS since gels were fabricated in confined molds without excess water. Hydrolytic degradation of the PAMAM amide bonds and DBA ester groups was accelerated by the basic pH, and the degradation timescale can ultimately be tuned through modulation of the PAMAM composition and molecular weight.

3.5 Hydrogel Swelling

The effects of different hydrogel parameters on the degree of post-formation syneresis and hydrogel stability were examined in a factorial swelling study. The parameters varied were the TGM polymer amount in the injectable solution (TGM wt %), functionality ratio between amine groups of the PAMAM and epoxy groups on the TGM (amine:epoxy mol ratio), the DBA mol content, and the molecular weight (MW) of the PAMAM crosslinker. It should be noted that the 1:1 amine:epoxy mol ratio corresponds to the theoretical maximum degree of crosslinking for each combination of TGM and PAMAM macromers studied.

The weight swelling ratio (q) of the hydrogels was measured at formation (24 h after fabrication in molds, q_f) and equilibrium (24 h after swelling in PBS at 37°C, q_s). Figure 5 shows the swelling capacity of the hydrogels in the factorial study. For all hydrogel formulations, formation swelling ratios for the 15 and 20 wt % groups were lower than that of the 10 wt % groups due to the higher polymer content. At equilibrium, the weight swelling ratios increased proportionately. The higher TGM wt % groups resisted further expansion due to their more tightly crosslinked network. Greater equilibrium swelling was also observed in the P-2600-containing formulations as well as the higher amine:epoxy ratio, indicating that the PAMAM MW and greater incorporation of branches contributed to the overall hydrophilicity and the subsequent swelling behavior.

To more extensively evaluate the effects and interactions of the four parameters (TGM wt %, amine:epoxy mol ratio, DBA mol content, and PAMAM MW) on hydrogel swelling behavior, a full 2^4 factorial analysis was performed. Table 3 lists the high/low values of each parameter.

The results were analyzed with SAS JMP v.10 software, and are illustrated in Figure 6, which shows the main effects of parameters at formation and equilibrium with error bars representing the standard error of each effect population. The zero line represents the overall population mean for each effect (5.20 ± 0.38 and 6.93 ± 0.37 for formation and equilibrium, respectively). TGM wt % (factor c), or polymer content of TGM, was the most significant factor at formation, the effect of which is maintained at equilibrium. Higher TGM wt % decreased swelling through reduced availability of water in the injected solution and a tightly crosslinked network that was resistant to further expansion. The other factors displayed a positive significant impact only at equilibrium, with increases in the PAMAM MW (factor b), DBA mol content (factor a), and amine:epoxy mol ratio (factor d) leading to greater equilibrium swelling by 0.56 ± 0.39, 0.94 ± 0.39, and 0.76 ± 0.39, respectively. All three parameters resulted in an increase in overall gel hydrophilicity due to higher total mol content of PAMAM (amine:epoxy mol ratio), higher PAMAM mass (PAMAM MW), or exposure of hydrophilic groups (DBA mol content). The DBA mol content was hypothesized to have a lesser effect than the other factors on formation and equilibrium swelling; however, the expedited degradation of the DBA on a rapid timescale to produce hydrophilic hydroxyl and carboxyl groups increased polymer hydrophilicity and contributed to its unexpected greater impact at equilibrium.

A number of significant cross interactions are also observed in the formation and equilibrium weight swelling ratios, which are illustrated in Figure 7. Although increasing DBA mol content only led to a significant main effect in equilibrium swelling, this effect

was enhanced by lower PAMAM MW at both formation and equilibrium (ab interaction). The higher swelling due to the increased gel hydrophilicity from the accelerated time-dependent hydrolysis of the DBA ring was likely initially offset for the lower PAMAM MW crosslinked hydrogels, which, due to their shorter crosslink interchain bridge length, reduced their capacity for subsequent expansion[32, 33]. This cross effect between high DBA mol content and lower PAMAM MW was additionally observed at formation with the lower TGM wt % (abc interaction). It was likely that the higher overall water content and greater expansion potential of the 10 wt %, P-2600 hydrogels coupled with the contribution of hydrophilic groups from hydrolyzed DBA led to a transient increased swelling response. At equilibrium, interaction effects were observed between higher final hydrophilicity and a more loosely-crosslinked network (ac interaction) due to the higher DBA mol content and lower TGM wt %. Finally, the cd interaction at formation between the PAMAM mol content (amine:epoxy ratio) and the TGM wt % was primarily a reflection of the reduced initial water content for the same volume of injected solution.

3.5 Mechanical Testing

Another factorial study was performed to examine the tunability of the mechanical behavior of the hydrogels. Unconfined compression testing was performed on 6 mm diameter × 3 mm height hydrogels with varying TGM wt % (10, 15, 20 wt %) and amine:epoxy mol ratio (0.5:1, 1:1). Using 6% DBA and 1440 Da PAMAM hydrogels, all the groups displayed an unconfined compressive modulus, E, in the kilopascal range, with the lowest modulus for the 10 wt % 0.5:1 crosslinked group at 1.72 kPa and highest modulus for the 15 wt % 1:1 crosslinked group at 7.26 kPA (Figure 8). The results indicate that higher TGM wt % (15 and 20 wt %) and higher crosslinking density led to significant increases in the Young's modulus. No significant differences were found between the different groups when the crosslinking density was halved (0.5:1 amine:epoxy mol ratio). The higher TGM wt % groups possessed a greater polymer density at the maximum crosslinking ratio, allowing for an increased compressive strength. However, at the lower amine:epoxy ratio, there was little dimensional stability, and the gels performed similarly under the compression test. Additionally, although the 15 wt % 1:1 crosslinking hydrogels demonstrated the highest modulus, there was not a significant difference between this group and the 20 wt % 1:1 crosslinking group.

3.6 Cytocompatibility Testing

The cytocompatibility of the hydrogel system was evaluated by treating rat fibroblast cells in media with 1, 10 and 100× dilutions of leachable products from the different TGM and crosslinked hydrogel formulations, or the degradation products from crosslinked hydrogel formulations, and incubating for 2 or 24 h at 37°C. Statistically significant differences were determined by a Tukey's test within time points and a t-test across time points ($p<0.05$). Leachables from the 10 and 20 wt % TGM hydrogels without PAMAM were found to be cytocompatible at all the conditions tested (Figure 9). The leachable products from the PAMAM crosslinked hydrogels demonstrated dose- and time-dependent cytocompatibility at the higher TGM wt % (1×) and lower crosslinker MW (P-1440). The reduced cytocompatibility for the 20 wt % P-1440 group can be attributed to the higher polymer concentration, which increases solution osmolality, and lower MW polymers, which may potentially interact with the cell membrane[34].

The degradation products from the hydrogel demonstrated short-term cytocompatibility at the higher dilutions, but produced significant decreases in cell viability for all dilutions at the later timepoint as a function of hydrogel polymer content, PAMAM MW, and degradation product dose (Figure 10). For all hydrogel formulations except the 10 wt % P-1440 group, a 1000× dilution group was added since cytotoxicitywas observed for the

100× dilution. Exposure to the lower MW products from the PAMAM crosslinker and formation of acidic groups from DBA hydrolysis is one possible explanation for the adverse response. However, the NaOH-catalyzed process to obtain the hydrogel degradation products also may have contributed to the decreased cell viability. The use of strong base to accelerate degradation introduced a significant amount of ions into the system, which could not be easily separated from the actual hydrogel degradation products.

In order to distinguish the effects between the hydrogel degradation products and the solution osmolality, osmometry was performed on NaCl-treated DMEM and the degradation product dilutions. Figure 11 illustrates the effect of increasing NaCl incorporation on DMEM osmolality and fibroblast viability after 24 h. Increasing the NaCl beyond 0 and 30 mg/10 mL DMEM, or an osmolality greater than 450 mOsm, led to significant decrease in cell viability after 24 h. In comparison, the 1× dilutions of the 10 wt % P-1440, 10 wt % P-2600, 20 wt % P-1440 and 20 wt % P-2600 groups were extrapolated to be 355 mOsm, 481 mOsm, 377 mOsm, and 539 mOsm, respectively. The 1× values were extrapolated from the other dilutions since the solutions were too concentrated to be measured by the instrument. Several values of solution osmolality observed here fall at the upper limits of the range tolerable by cells (~370–500 mOsm) established in the literature[35, 36], which has been shown to suppress cell proliferation[37] and induce apoptosis[38–40]. We postulate that the use of NaOH in the degradation process and administration of all degradation products at once contributed greatly to the negative response *in vitro*.

3.7 MSC Encapsulation

To examine the potential of the hydrogel system for cell delivery in bone tissue engineering applications, a preliminary encapsulation study was performed using rat MSCs at an encapsulation density of 10 million cells/mL for 1 and 7 days. MSCs were able to be successfully encapsulated within the hydrogel using media with serum, which did not negatively affect the crosslinking reactions of the hydrogel. The slight drop in cell viability after the initial week is consistent with MSC encapsulation in similar hydrogels in published studies[28] and the hydrogel was able to support live cells up to 7 days with homogenous distribution after encapsulation, as shown in Figure 12.

4. Conclusion

A novel injectable, thermally responsive, chemically crosslinkable, and bioresorbable hydrogel was successfully developed through the synthesis and combination of PNiPAAm-based thermogelling macromers with diamine-functionalized PAMAM crosslinkers. The system addresses the main challenges of using PNiPAAm-based hydrogels for tissue engineering, namely, post-formation syneresis and minimal resorbability, through the incorporation of a crosslinkable epoxy pendant group and hydrolyzable lactone ring. Hydrogel formation occurred through rapid thermogelation at 37°C and was stabilized through concomitant amine-epoxy chemical crosslinking over a period of 2 h, creating non-shrinking hydrogels. Additionally, hydrogel degradation was facilitated under accelerated conditions through hydrolysis-dependent processes. Hydrogel swelling was primarily controlled by the overall hydrophilicity and structure of the polymer network, modulated by the content of TGM and PAMAM crosslinker or DBA incorporation, or crosslinker length and density, respectively, while the unconfined compressive modulus was dependent on both the polymer concentration and extent of crosslinking. The leachable products from the hydrogel system were shown to be cytocompatible for the tested macromer and crosslinked hydrogel concentrations and timescales. Solution osmolality was the primary contributing factor towards the dose- and time-dependent response of the hydrogel degradation products. A preliminary encapsulation study suggested that MSCs could be successfully encapsulated

without affecting hydrogel crosslinking, and that the hydrogel could support cell viability for up to 7 days. The results suggest that the injectable, thermally and chemically crosslinking hydrogel system studied herein holds great potential for biomedical applications, especially for cell delivery in tissue engineering.

Supplementary Material

Refer to Web version on PubMed Central for supplementary material.

Acknowledgments

This work was funded by the National Institutes of Health (R01 DE017441), Baylor's Scientific Training Program for Dental Academic Researchers (T32 DE018380), and a Ruth L. Kirschstein fellowship from the National Institute of Dental and Craniofacial Research (F31 DE023999).

References

1. Slaughter BV, Khurshid SS, Fisher OZ, Khademhosseini A, Peppas NA. Adv. Mater. 2009; 21(32–33):3307–3329. [PubMed: 20882499]
2. Li Y, Rodrigues J, Tomas H. Chem. Soc. Rev. 2012; 41(6):2193–2221. [PubMed: 22116474]
3. Kretlow JD, Klouda L, Mikos AG. Adv. Drug Delivery Rev. 2007; 59(4–5):263–273.
4. Kretlow JD, Young S, Klouda L, Wong M, Mikos AG. Adv. Mater. 2009; 21(32–33):3368–3393. [PubMed: 19750143]
5. Vo TN, Kasper FK, Mikos AG. Adv. Drug Delivery Rev. 2012; 64(12):1292–1309.
6. Fong EL, Watson BM, Kasper FK, Mikos AG. Adv. Mater. 2012; 24(36):4995–5013. [PubMed: 22821772]
7. Schild HG. Prog. Polym. Sci. 1992; 17(2):163–249.
8. Hacker MC, Klouda L, Ma BB, Kretlow JD, Mikos AG. Biomacromolecules. 2008; 9(6):1558–1570. [PubMed: 18481893]
9. Na K, Park JH, Kim SW, Sun BK, Woo DG, Chung HM, Park KH. Biomaterials. 2006; 27(35):5951–5957. [PubMed: 16949668]
10. Uludag H, Norrie B, Kousinioris N, Gao TJ. Biotechnol. Bioeng. 2001; 73(6):510–521. [PubMed: 11344456]
11. Stile RA, Healy KE. Biomacromolecules. 2001; 2(1):185–194. [PubMed: 11749171]
12. Ekenseair AK, Kasper FK, Mikos AG. Adv. Drug Delivery Rev. 2012; 65(1):89–92.
13. Ma ZW, Nelson DM, Hong Y, Wagner WR. Biomacromolecules. 2010; 11(7):1873–1881. [PubMed: 20575552]
14. Neradovic D, van Steenbergen MJ, Vansteelant L, Meijer YJ, van Nostrum CF, Hennink WE. Macromolecules. 2003; 36(20):7491–7498.
15. Fujimoto KL, Ma ZW, Nelson DM, Hashizume R, Guan JJ, Tobita K, Wagner WR. Biomaterials. 2009; 30(26):4357–4368. [PubMed: 19487021]
16. Sun LF, Zhuo RX, Liu ZL. Macromol. Biosci. 2003; 3(12):725–728.
17. Yoshida T, Aoyagi T, Kokufuta E, Okano T. J. Polym. Sci., Part A: Polym. Chem. 2003; 41(6):779–787.
18. Rosellini E, Cristallini C, Guerra GD, Barbani N, Giusti P. Biomed. Mater. 2010; 5(3):1–9.
19. Cui ZW, Lee BH, Pauken C, Vernon BL. J. Biomater. Sci., Polym. Ed. 2010; 21(6–7):913–926. [PubMed: 20482992]
20. Cui ZW, Lee BH, Vernon BL. Biomacromolecules. 2007; 8(4):1280–1286. [PubMed: 17371066]
21. Ekenseair AK, Boere KWM, Tzouanas SN, Vo TN, Kasper FK, Mikos AG. Biomacromolecules. 2012; 13(9):2821–2830. [PubMed: 22881074]
22. Ekenseair AK, Boere KWM, Tzouanas SN, Vo TN, Kasper FK, Mikos AG. Biomacromolecules. 2012; 13(6):1908–1915. [PubMed: 22554407]

23. Fitzpatrick SD, Jafar Mazumder MA, Muirhead B, Sheardown H. Acta Biomater. 2012; 8:2517–2528. [PubMed: 22426139]
24. Standardization, IOo. ISO10993-13: Biological Evaluation of Medical Devices: Identification and quantification of degradation products from polymeric medical devices. Geneva: Switzerland;
25. Shin H, Temenoff JS, Mikos AG. Biomacromolecules. 2003; 4(3):552–560. [PubMed: 12741769]
26. Timmer MD, Shin H, Horch RA, Ambrose CG, Mikos AG. Biomacromolecules. 2003; 4(4):1026–1033. [PubMed: 12857088]
27. Klouda L, Hacker MC, Kretlow JD, Mikos AG. Biomaterials. 2009; 30(27):4558–4566. [PubMed: 19515420]
28. Klouda L, Perkins KR, Watson BM, Hacker MC, Bryant SJ, Raphael RM, Kasper FK, Mikos AG. Acta Biomater. 2011; 7(4):1460–1467. [PubMed: 21187170]
29. Hennink WE, van Nostrum CF. Adv. Drug Delivery Rev. 2012; 64:223–236.
30. Mijovic J, Fishbain A, Wijaya J. Macromolecules. 1992; 25(2):986–989.
31. Vyazovkin S, Sbirrazzuoli N. Macromolecules. 1996; 29(6):1867–1873.
32. Ekenseair AK, Peppas NA. AIChE J. 2012; 58(5):1600–1609.
33. Ekenseair AK, Peppas NA. Polymer. 2012; 53(18):4010–4017.
34. Vihola H, Laukkanen A, Valtola L, Tenhu H, Hirvonen J. Biomaterials. 2005; 26(16):3055–3064. [PubMed: 15603800]
35. Racz B, Reglodi D, Fodor B, Gasz B, Lubics A, Gallyas F Jr, Roth E, Borsiczky B. Bone. 2007; 40(6):1536–1543. [PubMed: 17392049]
36. Friis MB, Friborg CR, Schneider L, Nielsen MB, Lambert IH, Christensen ST, Hoffmann EK. J. Physiol. 2005; 567(Pt 2):427–443. [PubMed: 15975986]
37. Kim NS, Lee GM. J. Biotechnol. 2002; 95(3):237–248. [PubMed: 12007864]
38. Criollo A, Galluzzi L, Maiuri MC, Tasdemir E, Lavandero S, Kroemer G. Apoptosis. 2007; 12(1):3–18. [PubMed: 17080328]
39. Han YK, Kim YG, Kim JY, Lee GM. Biotechnol. Bioeng. 2010; 105(6):1187–1192. [PubMed: 20014438]
40. Mockridge JW, Benton EC, Andreeva LV, Latchman DS, Marber MS, Heads RJ. Biochem. Biophys. Res. Commun. 2000; 273(1):322–327. [PubMed: 10873605]

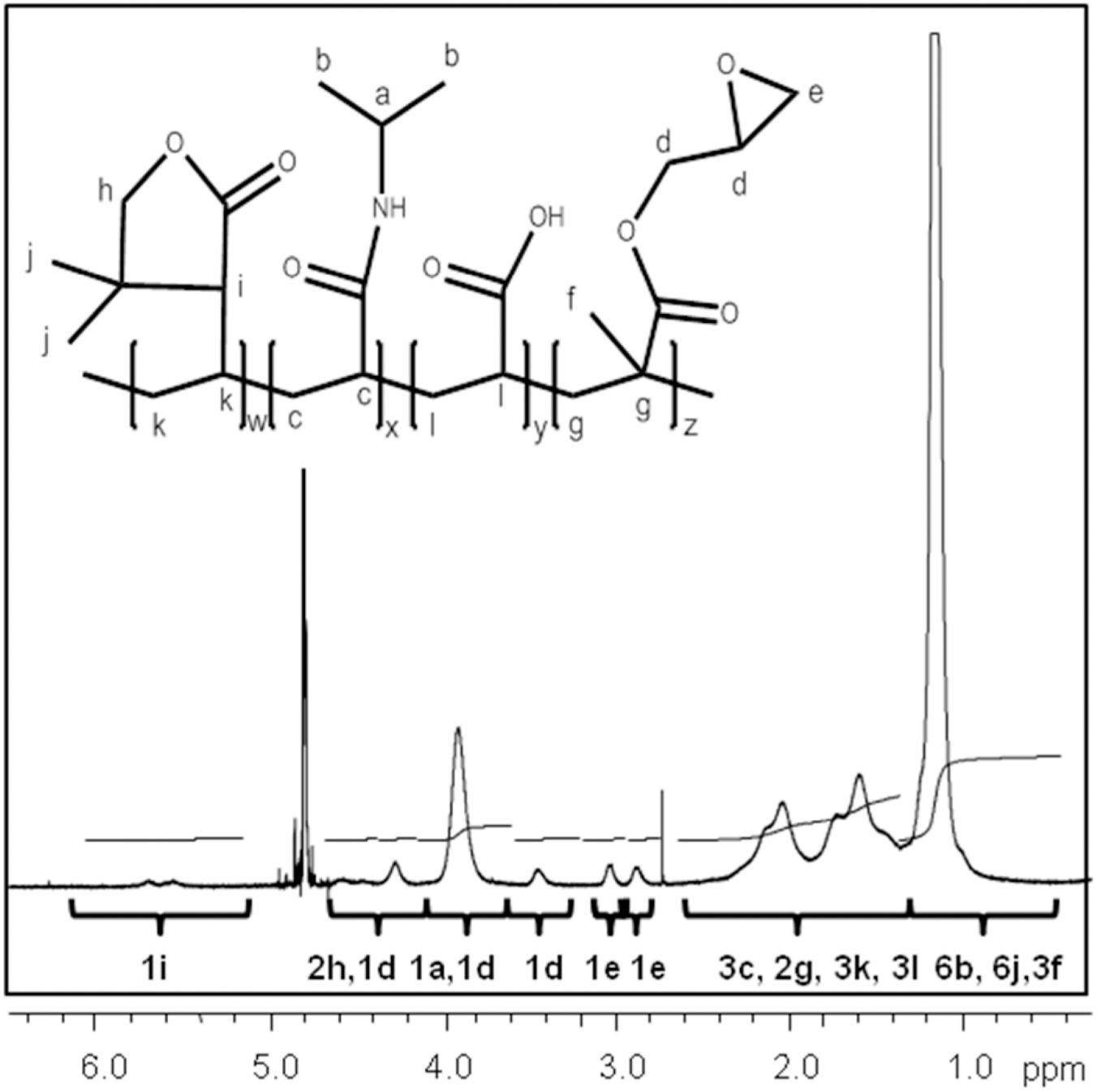

Figure 1.

^{1}H NMR spectrum of P(NiPAAm-*co*-GMA-*co*-DBA-*co*-AA) TGM. Peak proton locations are identified with letters a–l.

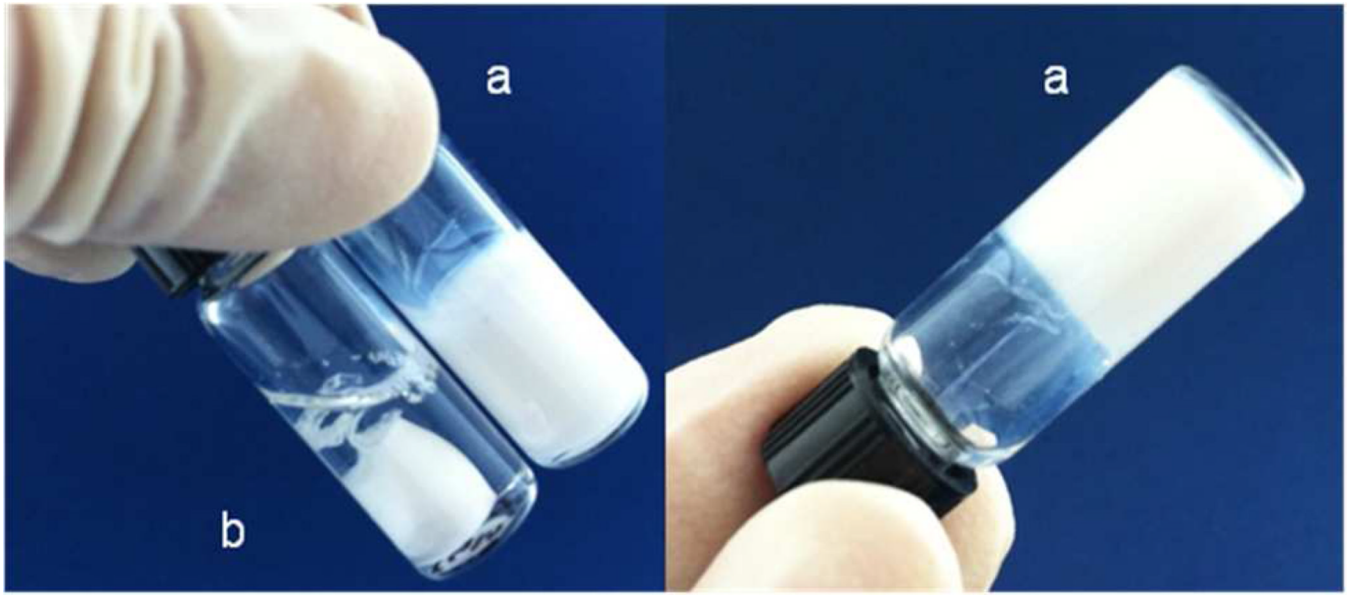

Figure 2.
Thermogelation of 10 wt % TGM containing 6 mol % DBA with (a) and without (b) addition of P-1440 PAMAM after one minute at 37°C.

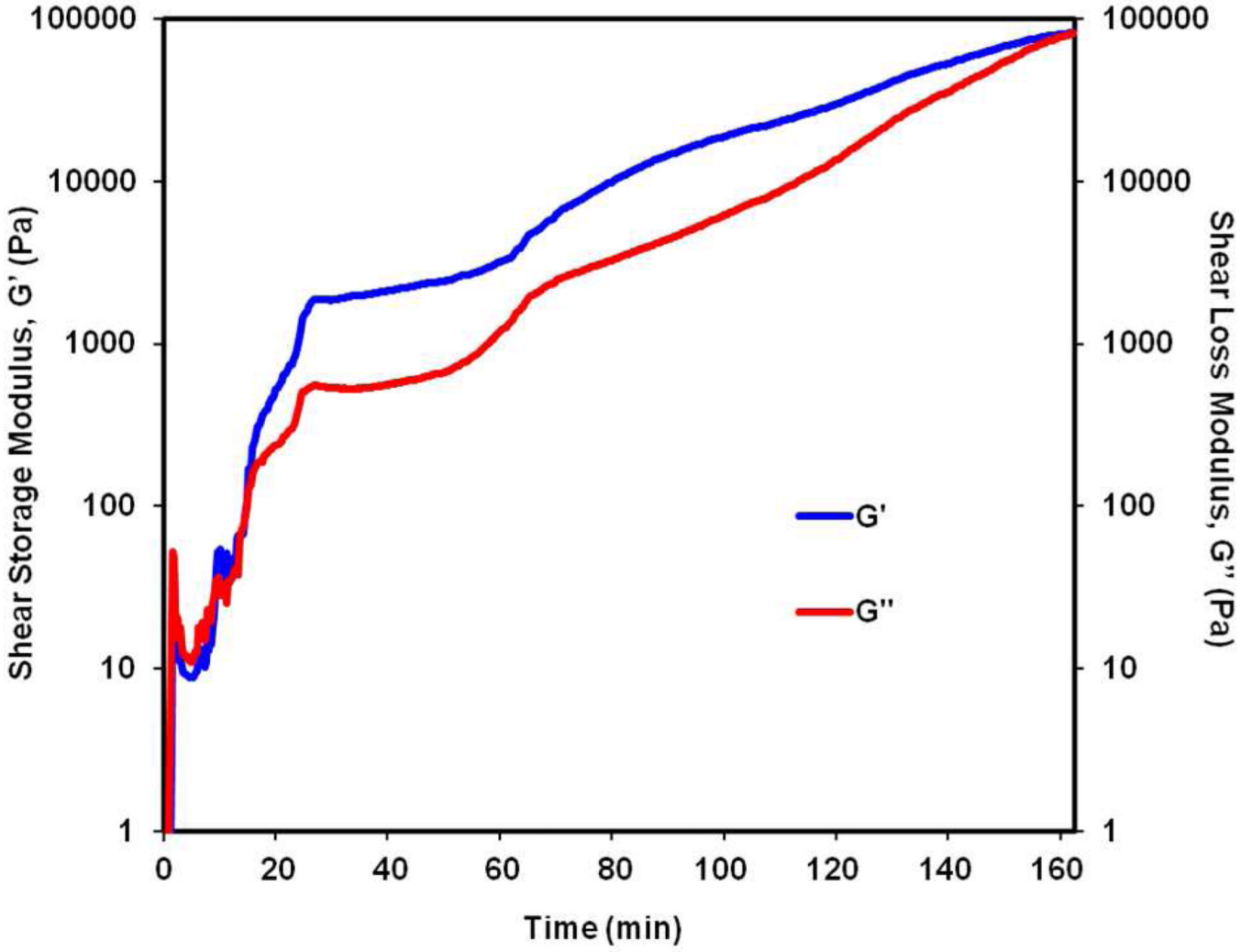

Figure 3.
Oscillatory rheology trace showing shear storage (G') and loss (G") moduli for a 10 wt % hydrogel composition containing 6 mol % DBA crosslinked with P-1440 PAMAM at 1:1 amine:epoxy ratio held at 4°C for 1 min and then 37°C for 3 h.

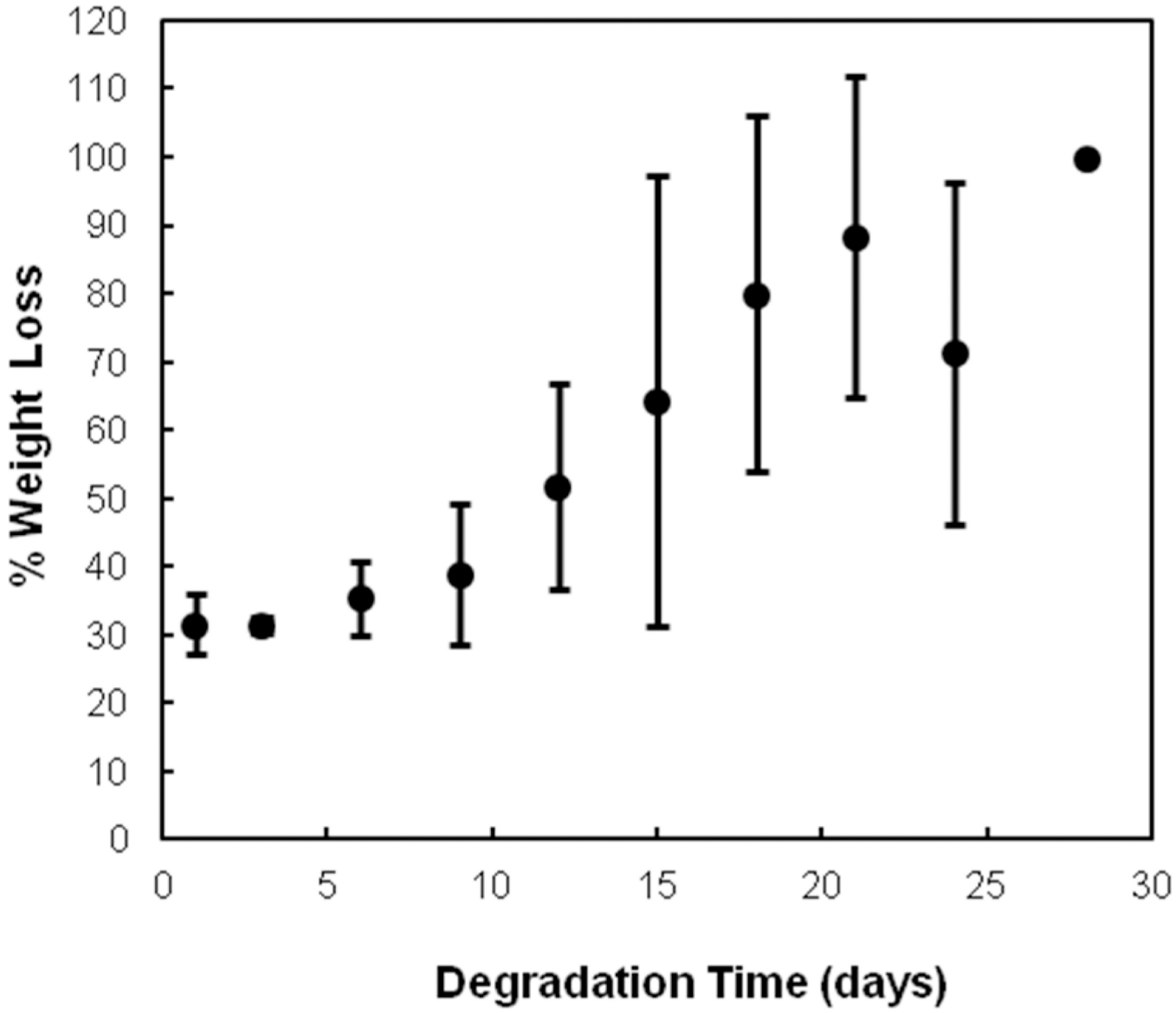

Figure 4.
Degradation profile of a 10 wt % hydrogel with 6 mol % DBA crosslinked with P-1440 PAMAM at 1:1 amine:epoxy ratio under accelerated conditions (pH = 10.5 at 70°C). Data are reported as means ± standard deviation for a sample size of n = 4.

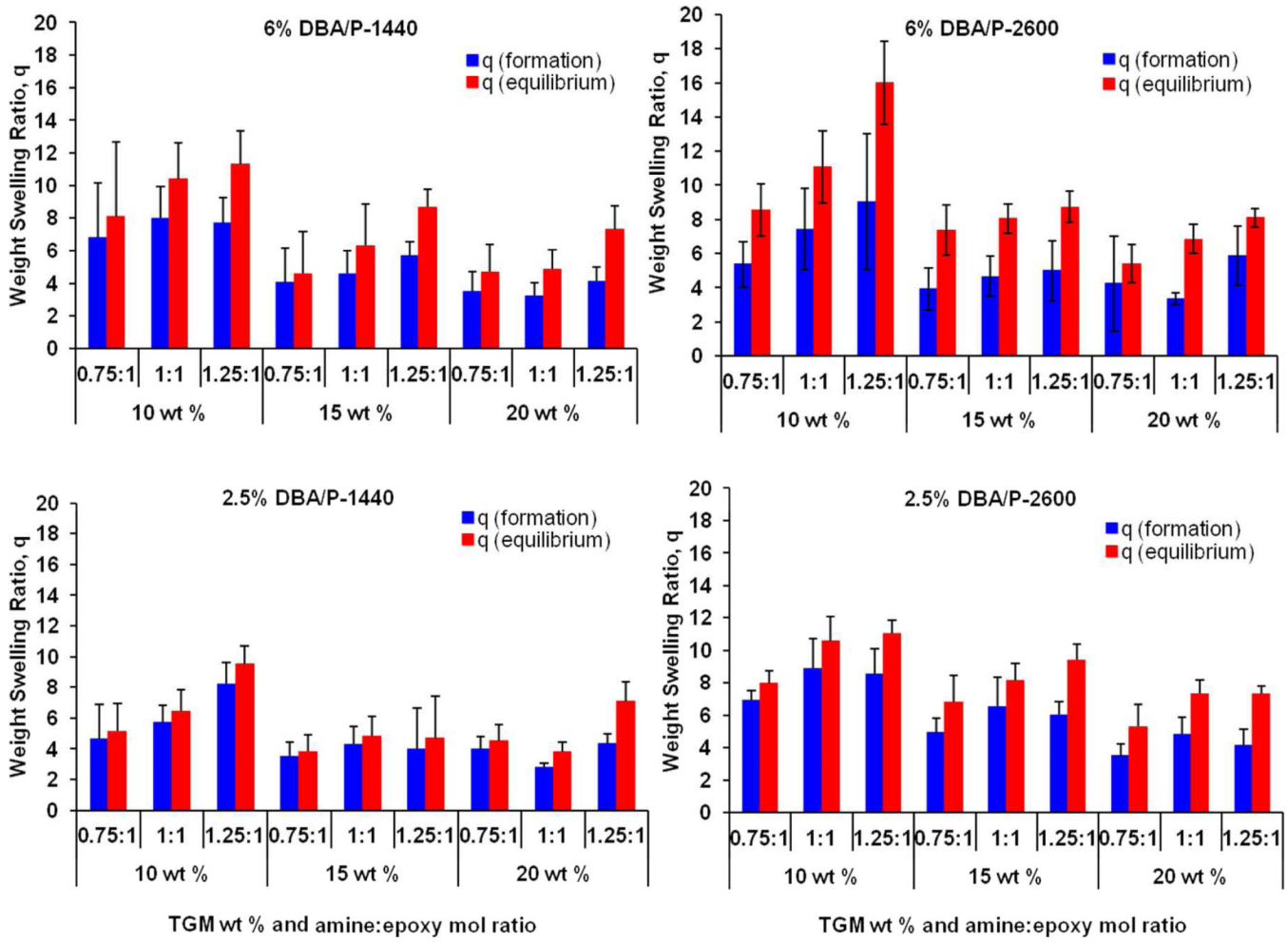

Figure 5.

Formation and equilibrium weight swelling ratio of 36 different hydrogel formulations (6 mm in diameter, 3 mm in height) in a factorial study. Hydrogels vary in DBA mol content (2.5% or 6%), PAMAM molecular weight (1440 Da or 2600 Da), amine:epoxy mol ratio (0.75:1, 1:1, or 1.25:1), and TGM wt % (10, 15 or 20 wt %) in PBS pH 7.4 at 37°C. Data are reported as means ± standard deviation for a sample size of n = 4–6.

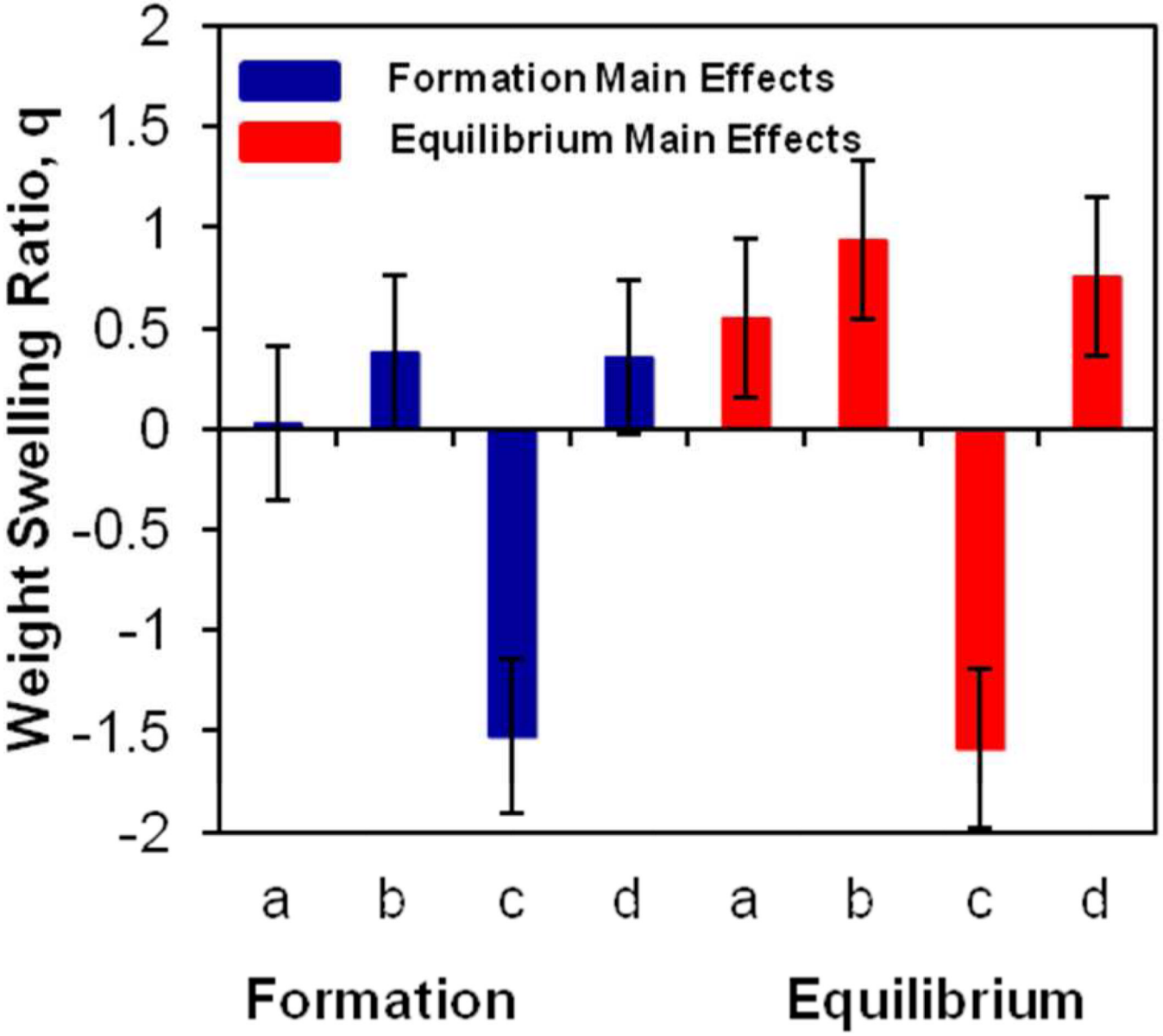

Figure 6.
Main effects for formation and equilibrium weight swelling ratios from 2^4 full factorial study. The effects a, b, c, and d correspond to the parameters DBA mol content, PAMAM molecular weight, TGM wt %, and amine:epoxy mol ratio, respectively. The error bars represent the standard error from the overall population mean. Significant effects are indicated by error bars that do not cross the x-axis.

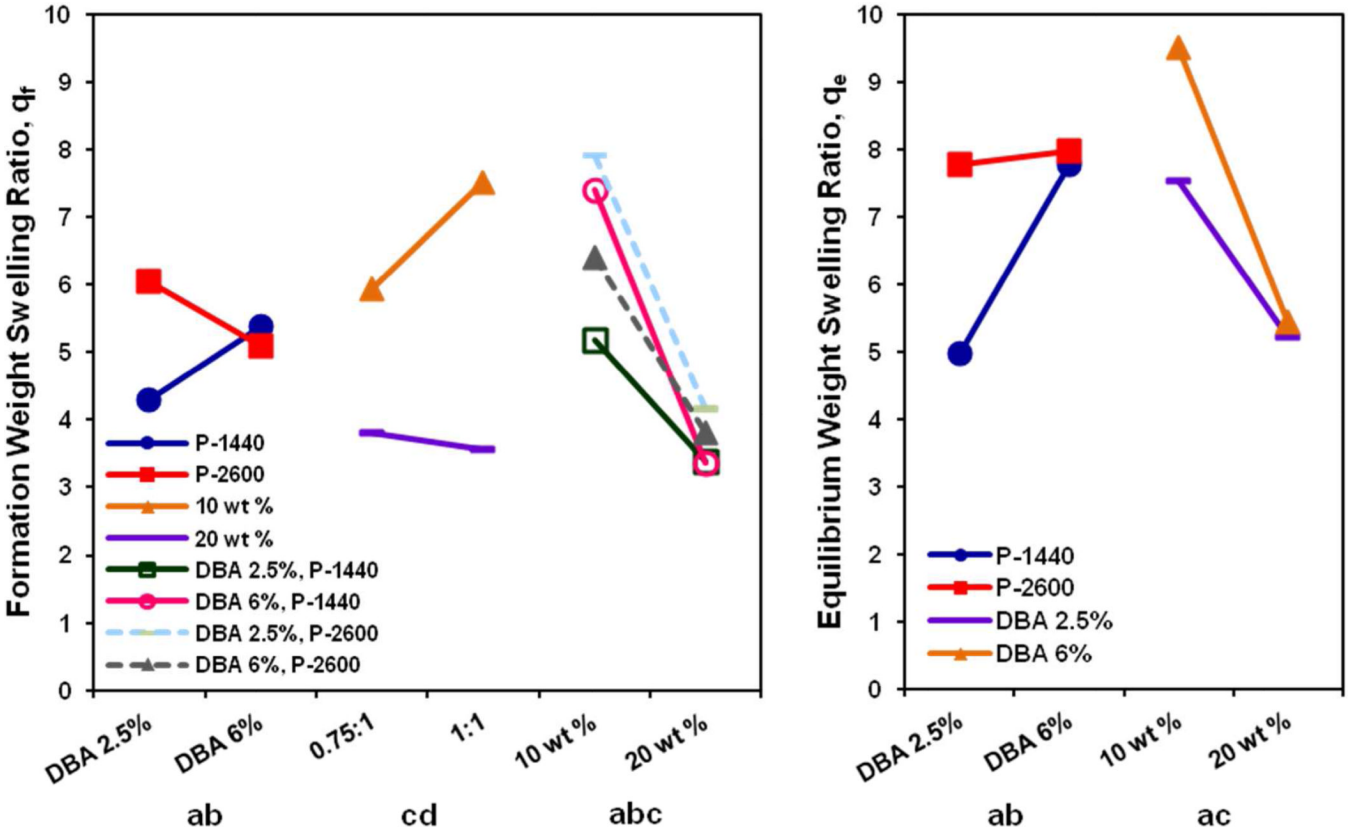

Figure 7.
Statistically significant interaction effects between DBA mol content (a), PAMAM MW (b), TGM wt % (c), and amine:epoxy mol ratio (d) on the formation (left) and equilibrium (right) weight swelling ratio of hydrogels from the 2^4 factorial experimental design.

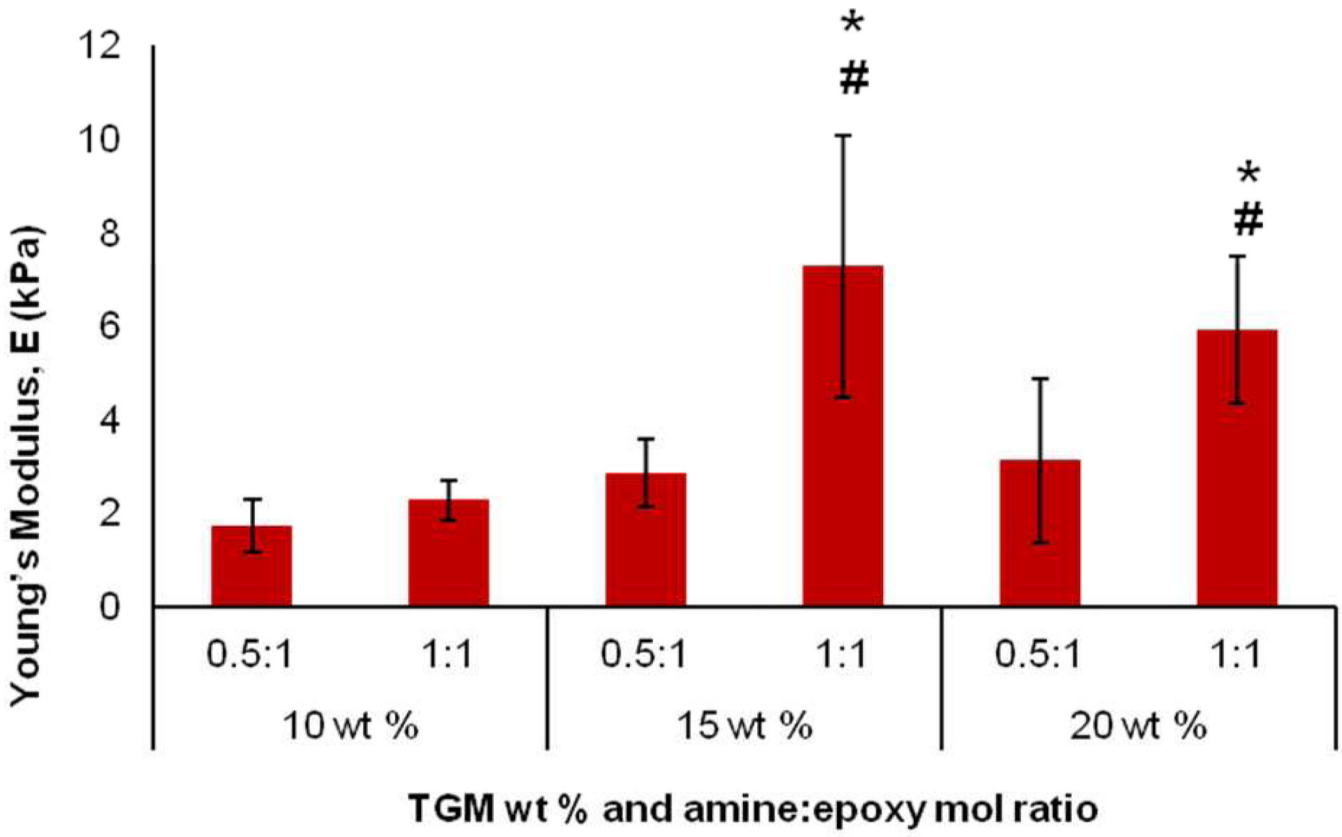

Figure 8.
Unconfined compressive Young's modulus of 6 mol % DBA-containing hydrogels crosslinked with P-1440 PAMAM (6 mm in diameter, 3 mm in height) with varying TGM wt % and amine:epoxy mol ratio. Data are reported as means ± standard deviation for a sample size of n = 6. * and # indicate statistical significance from 10 wt % group at the same amine:epoxy mol ratio and within same TGM wt % at different amine:epoxy mol ratio, respectively.

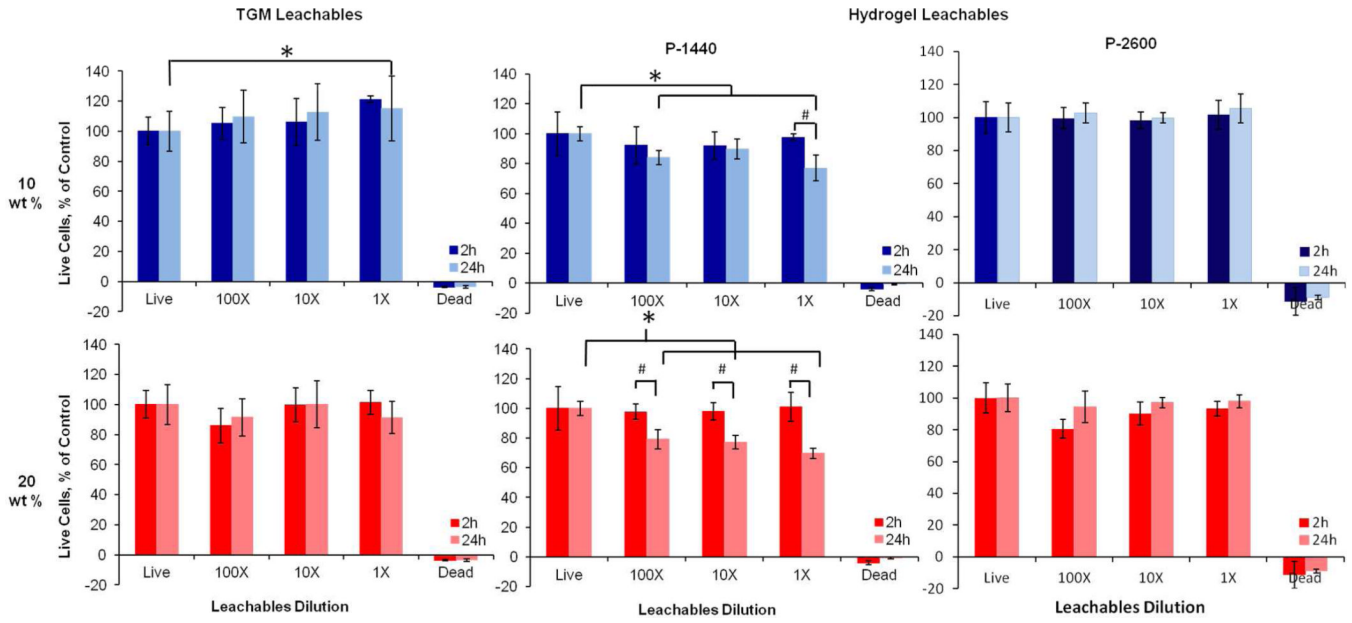

Figure 9.

Viability of rat fibroblasts in *in vitro* cytocompatibility testing of TGM and hydrogel leachable products with 6 mol % DBA at 2 and 24 h. The first column corresponds to TGM leachables, and the second and third columns correspond to hydrogel leachables with P-1440 and P-2600 crosslinker, respectively. The top and bottom rows refer to 10 or 20 wt % hydrogels, respectively. Data are reported as means ± standard deviation for a sample size of n = 6. * and # indicate statistical significance ($p<0.05$) within and between timepoints, respectively.

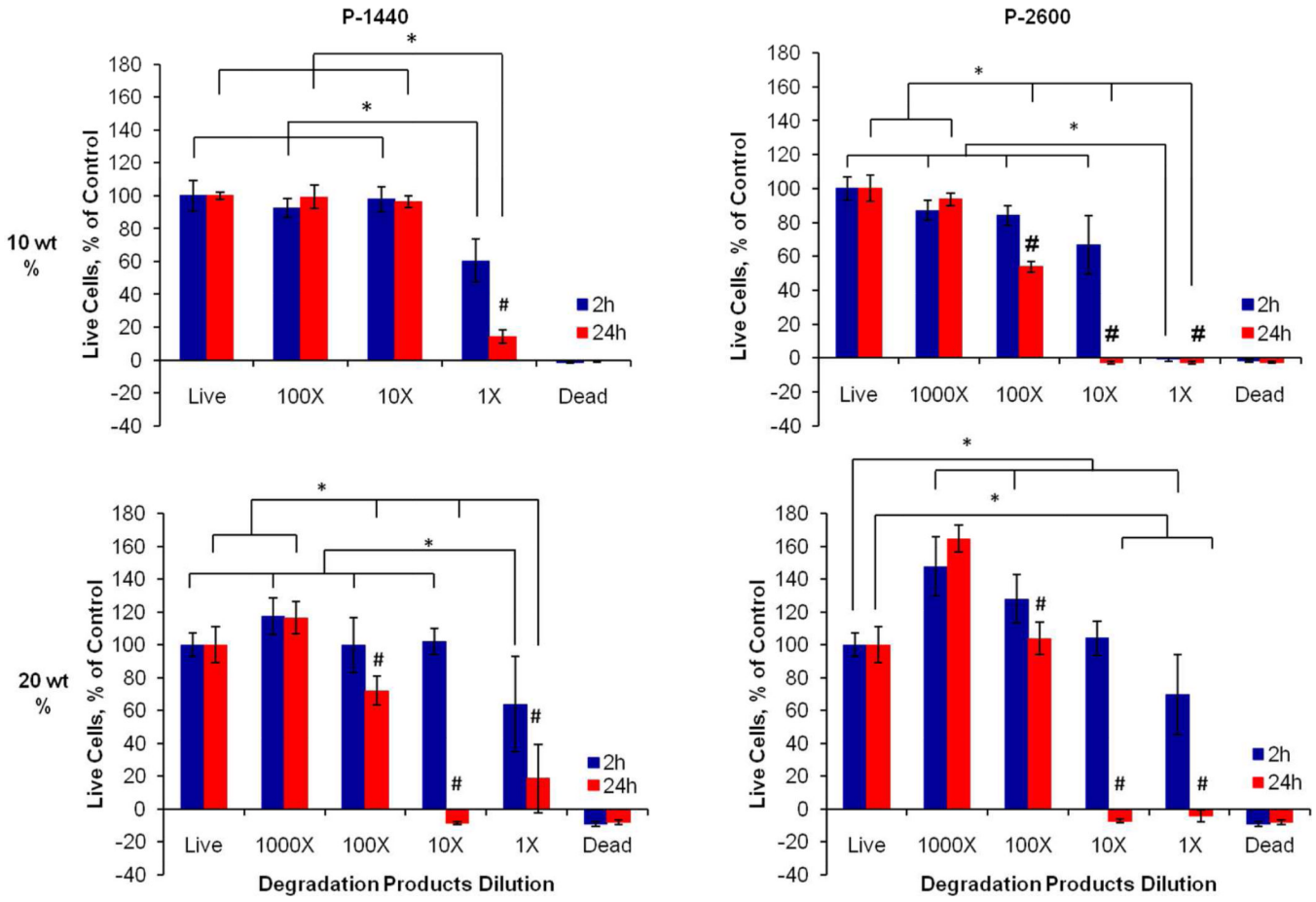

Figure 10.

Viability of rat fibroblasts in *in vitro* cytocompatibility testing of 6 mol % DBA-containing hydrogel degradation products. Rows correspond to the hydrogel TGM wt % (10 or 20 wt %), while columns refer to the PAMAM crosslinker used at a 1:1 amine:epoxy mol ratio (P-1440 or P-2600). Data are reported as means ± standard deviation for a sample size of n = 6. * and # indicate statistical significance ($p<0.05$) within and between timepoints, respectively.

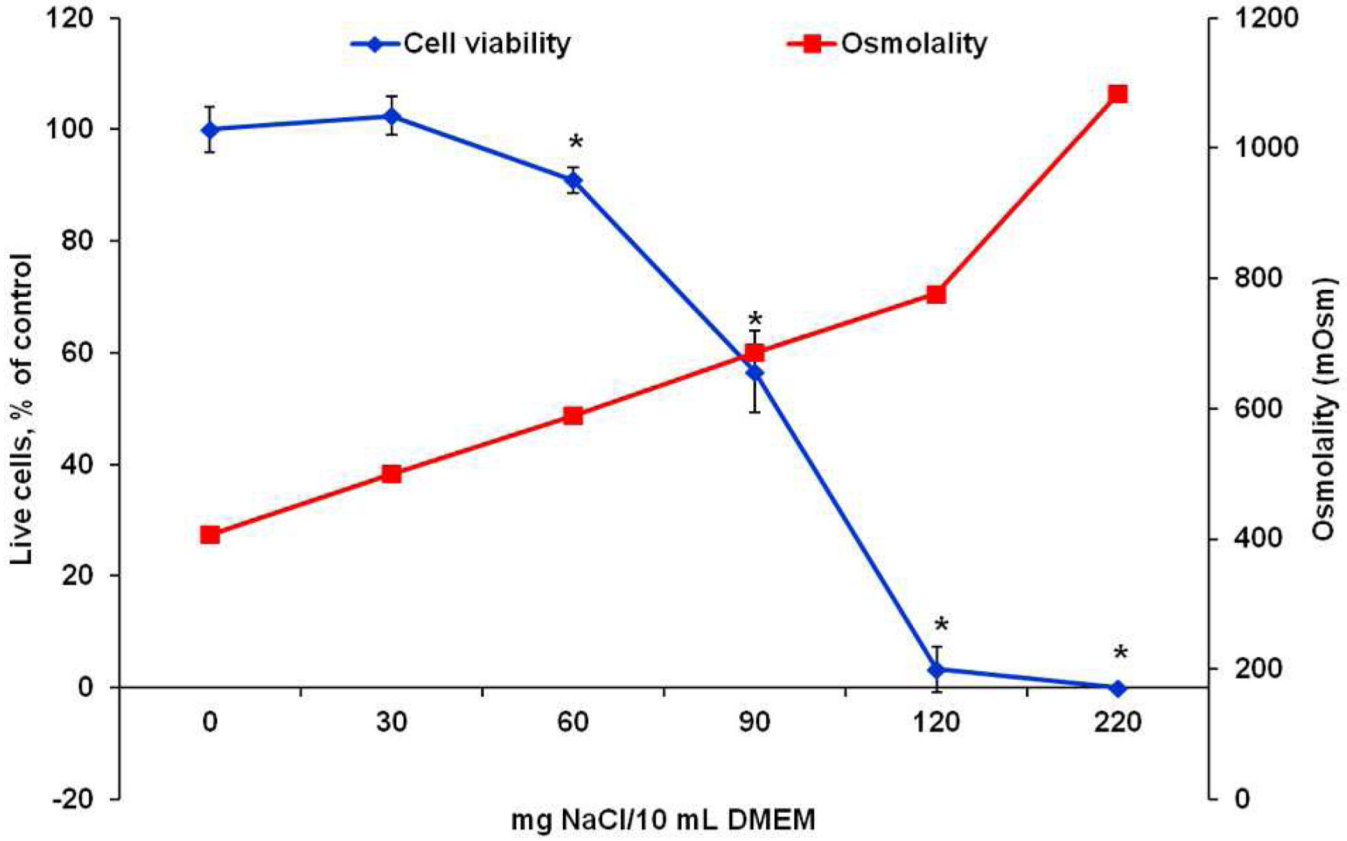

Figure 11.

Osmolality of 0, 30, 60, 90, 120, and 220 mg NaCl/10 mL DMEM solutions and cell viability after incubation with the solutions after 24 h. * marks statistical differences in cell viability from the 0 and 30 mg NaCl/10 mL DMEM groups ($p<0.05$).

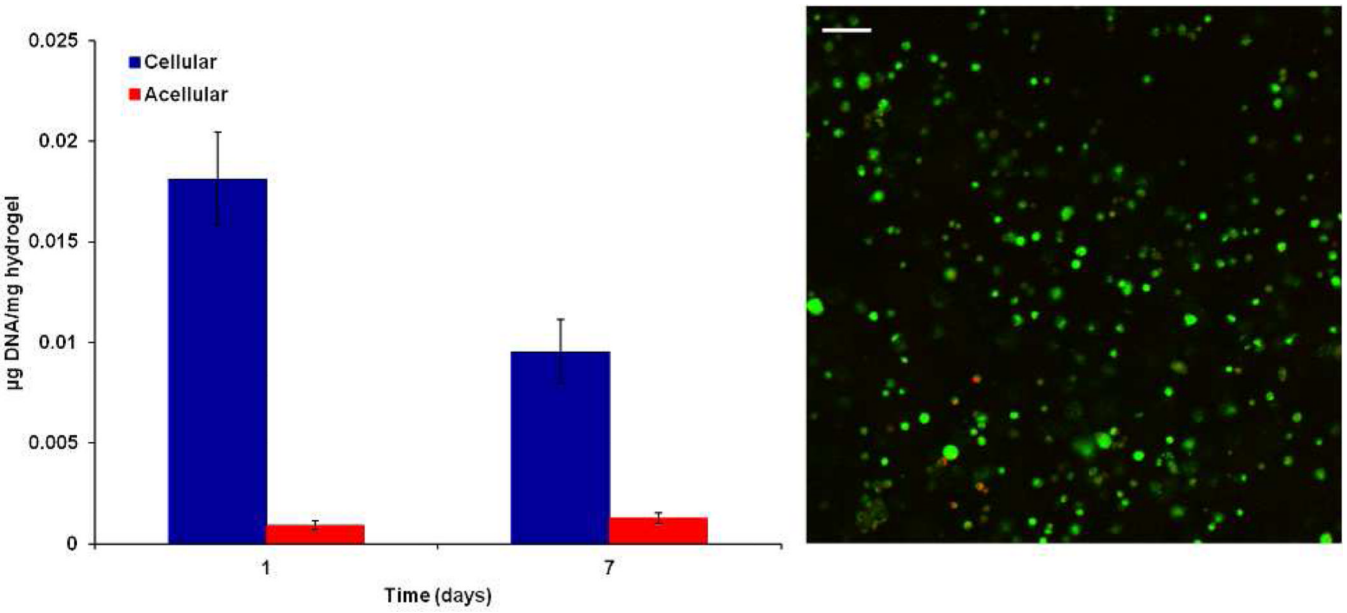

Figure 12.

DNA content of acellular and cellular 10 wt % hydrogels with predifferentiated MSCs at an encapsulation density of 10 million cells/mL hydrogel at 1 and 7 days. A representative confocal micrograph of a cellular hydrogel with Live/Dead staining at 7 days. Green and red staining indicate live or dead cells, respectively. Data are reported as means ± standard deviation for a sample size of n = 4. The scale bar represents 100 μm.

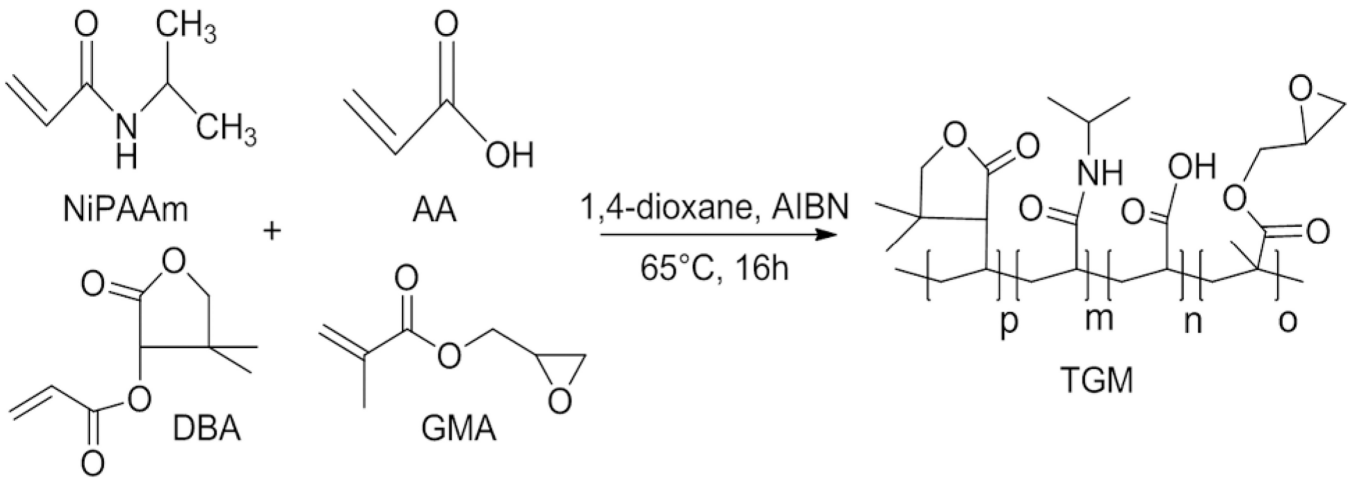

Scheme 1.

Synthesis of P(NiPAAm-*co*-GMA-*co*-DBA-*co*-AA) thermogelling macromer (TGM) via radical copolymerization of *N*-isopropylacrylamide (NiPAAm), glycidyl methacrylate (GMA), dimethyl-γ-butyrolactone acrylate (DBA), and acrylic acid (AA).

Table 1

TGM Synthesis and Thermal Characteristics

TGM	Feed Ratio (mol %)				Chemical Composition (mol %via NMR)				Initial Peak LCST [°C]	Hydrolysis Peak LCST [°C]
	pNiPAAm	GMA	DBA	AA	pNiPAAm	GMA	DBA	AA		
DBA-6	80.5	7.5	7	5	84.9 ± 0.06	9.1 ± 0.35	5.8 ± 0.26	3.2 ± 0.32	22.4 ± 1.0	63.3 ± 3.7
DBA-2.5	86.5	7.5	3.5	2.5	86.5 ± 0.20	7.0 ± 0.51	2.5 ± 0.28	3.5 ± 0.36	27.7 ± 0.1	39.5 ± 3.6

Table 2

Characterization of Synthesized PAMAM Crosslinkers

PAMAM	Stoichiometric Feed Ratio (r)	M_n (Da)	M_w (Da)	PDI
P-1440	0.78	1450	1990	1.38
P-2600	0.85	2580	3370	1.31

Table 3

Hydrogel Formulation Parameters for Full 2^4 Factorial Design

	DBA mol content	PAMAM MW	TGM wt %	Amine: epoxy mol ratio
high (+)	6%	2600	20 wt %	1:1
low (−)	2.5%	1440	10 wt %	0.75:1
Group	**a**	**b**	**c**	**d**
(1)	−	−	−	−
a	+	−	−	−
b	−	+	−	−
c	−	−	+	−
d	−	−	−	+
ab	+	+	−	−
ac	+	−	+	−
ad	+	−	−	+
bc	−	+	+	−
bd	−	+	−	+
cd	−	−	+	+
abc	+	+	+	−
abd	+	+	−	+
acd	+	−	+	+
bcd	−	+	+	+
abcd	+	+	+	+